

## Swarm Level 2 Processing System

### Intermediate validation of Swarm Level 2 Lithospheric Field Product

SW\_OPER\_MLI\_VALi2C\_00000000T000000\_99999999T999999\_0501

By: DTU

Date: 2019-02-26

### Abstract and Conclusion

The processes and tests applied in the intermediate validation of the MLI\_SHAi2C product

**SW\_OPER\_MLI\_SHAi2C\_00000000T000000\_99999999T999999\_0501**

and the conclusions on the product quality drawn herefrom are described in this document.

This product contains the representation of a model of the magnetic field of Earth's lithosphere ("crust") ("MLI" part of product name) using spherical harmonic coefficients ("SHA" part of product name). The model is estimated from Swarm and observatory data using the *Comprehensive Inversion* (CI) scheme within the Swarm Level 2 Processing system ("2C" part of product name). Operational Swarm Level 1b data version 0505 and 0506, covering the period from 2013-11-25 to 2018-12-31 are used for the model estimation; the product is considered static i.e. valid at all times ("00000000T000000\_99999999T999999" part of product name). This is version 0501 of the product (last part of product name), i.e. baseline 05 indicating 5<sup>th</sup> year CI production, first, minor version. The format of the product is described in "Product Specification for L2 Products and Auxiliary Products", doc. no. SW-DS-DTU-GS-0001.

The assessment of the SW\_OPER\_MLI\_SHAi2C\_00000000T000000\_99999999T999999\_0501 product shows good agreement with other lithospheric field models such as MF7 [Maus et.al., G3, 2010] and LCS-1 [Olsen et.al., GJI, 2017].

**The DTU SIL's opinion is that the MLI\_SHAi2C product is successfully validated and therefore suitable for release.**

# Swarm Level 2 Processing System

## Table of Contents

<b>1</b>	<b>Intermediate Validation Report of MLI_SHAi2C</b>	<b>5</b>
1.1	Input Data Products	5
1.2	Model Parameterization and Data Selection	5
1.3	Output Products	5
1.4	Validation Results	6
1.4.1	Spatial Power Density	6
1.4.2	Normalized Spherical Harmonic Coefficient Differences	7
1.4.3	Visualisation of Spatial Differences	8
1.4.4	Visualisation of Radial Field	9
1.4.5	Statistics of Model Residuals	9
1.5	Criteria	10
<b>2</b>	<b>Additional Information</b>	<b>11</b>
2.1	Model Configuration and Data Selection Parameters	11
2.2	Comments from Scientists in the Loop	12
2.2.1	Derivation of Model	12
2.2.2	Conclusion	12
<b>Annex A</b>	<b>Definitions of Tests</b>	<b>13</b>
A.1	Mean square vector field difference per spherical harmonic degree	13
A.2	Correlation per spherical harmonic degree	13
A.3	Visualisation of coefficient differences	13
A.4	Visualisation of spatial differences	14

# Swarm Level 2 Processing System

## Table of Figures

Figure 1-1: Spatial power densities and degree correlations	6
Figure 1-2: Normalized coefficient differences in percent	7
Figure 1-3: Spatial visualization of $B_r$ differences between CIY4 and LCS-1 models	8
Figure 1-4: Spatial visualization of $B_r$ of the CIY4 model	9

## Table of Tables

Table 1-1: Input data products	5
Table 1-2: Statistics of model residuals	10
Table 1-3: Validation criteria	10
Table 2-1: Model Configuration	12

## Abbreviations

<i>Acronym</i>	<i>Description</i>
CI	Comprehensive Inversion
CIY4	Comprehensive Inversion, Year 4
CIY5	Comprehensive Inversion, Year 5
L2PS	Level 2 Processing System
MLI	Magnetic Lithospheric field
SHA	Spherical Harmonic Analysis
SIL	Scientist in the Loop
STR	Star Tracker
VAL	Validation
VFM	Vector Field Magnetometer

# Swarm Level 2 Processing System

## References

- [Finlay et.al., EPS, 2016] *Recent geomagnetic secular variation from Swarm and ground observatories as estimated in the CHAOS-6 geomagnetic field model*; Finlay, Christopher C.; Olsen, Nils; Kotsiaros, Stavros; Gillet, Nicolas; Tøffner-Clausen, Lars; *Earth, Planets and Space*, Vol 68, 112 (2016). doi: [10.1186/s40623-016-0486-1](https://doi.org/10.1186/s40623-016-0486-1)
- [Maus et.al., G3, 2010] *Magnetic field model MF7*; Maus, Stefan, G3 (2010)
- [Olsen et.al., GJI, 2017] *LCS-1: A high-resolution global model of the lithospheric magnetic field derived from CHAMP and Swarm satellite observations*; Olsen, Nils; Ravat, ; Finlay, Christopher C.; Kother, Livia K.; *Geophysical Journal Int.*, Vol 211(3) (2017). doi: <http://dx.doi.org/10.1093/gji/ggx381>
- [Sabaka et.al., GRL, 2016] *Extracting Ocean-Generated Tidal Magnetic Signals from Swarm Data through Satellite Gradiometry*; Sabaka, Terence J. ; Tyler, Robert H. ; Olsen, Nils in journal: *Geophysical Research Letters* (ISSN: 0094-8276, 2016), doi: [10.1002/2016GL068180](https://doi.org/10.1002/2016GL068180)
- [Sabaka et.al., EPS, 2018] *A Comprehensive Model of Earth's Magnetic Field Determined From 4 Years of Swarm Satellite Observation*; Sabaka, Terence J. ; Tøffner-Clausen, Lars; Olsen, Nils; Finlay, Christopher C. *Earth Planets and Space*, in preparation (2018).

# Swarm Level 2 Processing System

## 1 Intermediate Validation Report of MLI\_SHAi2C

### 1.1 Input Data Products

The following input data products were used for the estimation of the MLI\_SHAi2C lithospheric field model

Products	Type	Period	Comment
SW_OPER_Q3D_CI_i2__0000000T000000_9999999T999999_0101	Q-matrix of Earth's (1-D mantle + oceans)	-	Used for computing induced part of ionospheric field
SW_OPER_AUX_OBS_2__20130101T000000_20131231T235959_0117 SW_OPER_AUX_OBS_2__20140101T000000_20141231T235959_0117 SW_OPER_AUX_OBS_2__20150101T000000_20151231T235959_0117 SW_OPER_AUX_OBS_2__20160101T000000_20161231T235959_0117 SW_OPER_AUX_OBS_2__20170101T000000_20171231T235959_0117 SW_OPER_AUX_OBS_2__20180101T000000_20181231T235959_0117	Observatory hourly mean values	2013-11-25 - 2017-10-31	A total of 163 observatories are included
SW_OPER_AUX_DST_2__19980101T013000_20190115T233000_0001 SW_OPER_AUX_F10_2__20060101T000000_20190115T000000_0001 SW_OPER_AUX_KP_2__19990101T023000_20190117T133000_0001	Indices	As indicated by the file names	
SW_OPER_MAGA_LR_1B_YYYYMMDDTh1m1s1_YYYYMMDDTh2m2s2_vvvv SW_OPER_MAGB_LR_1B_YYYYMMDDTh1m1s1_YYYYMMDDTh2m2s2_vvvv SW_OPER_MAGC_LR_1B_YYYYMMDDTh1m1s1_YYYYMMDDTh2m2s2_vvvv	Swarm magnetic data, 1 Hz	2013-11-25 - 2018-12-31	Decimated to 30 second sampling vvvv = 0505 or 0506

Table 1-1: Input data products

### 1.2 Model Parameterization and Data Selection

See Section 2.1.

### 1.3 Output Products

The products of this validation report are:

*Swarm Level 2 Magnetic Lithospheric field Product:*

SW\_OPER\_MLI\_SHAi2C\_0000000T000000\_9999999T999999\_0501

*Swarm Level 2 Intermediate Validation Product:*

SW\_OPER\_MLI\_VAL\_0000000T000000\_9999999T999999\_0501

# Swarm Level 2 Processing System

## 1.4 Validation Results

The tests were conducted between 2019-01-15 and 2018-02-10.

This 5<sup>th</sup> year CI L2 production, denoted CIY5, is very similar in methodology and results as last year's production (CIY4) which is thoroughly described in [Sabaka et.al., EPS, 2018]. The following contains the results of the tests performed on the lithospheric field output product. See Annex A for general definitions of various tests.

### 1.4.1 Spatial Power Density

Figure 1-1 below shows on the left the spatial power densities of the CIY5 and LCS-1 [Olsen et.al., GJI, 2017] lithospheric field models in blue and red respectively; and the power of the differences between the CIY5 model and LCS-1 (orange) and MF7 (purple). The differences are everywhere well below the actual field. As of degree ca. 80, the power of the CIY5 model is slightly larger than that of LCS-1 which might be due to measurement noise. On the right in Figure 1-1, the degree correlation between CIY5 and the two other models are plotted. The degree correlation with both is above 0.8 to above spherical harmonic degree 105.

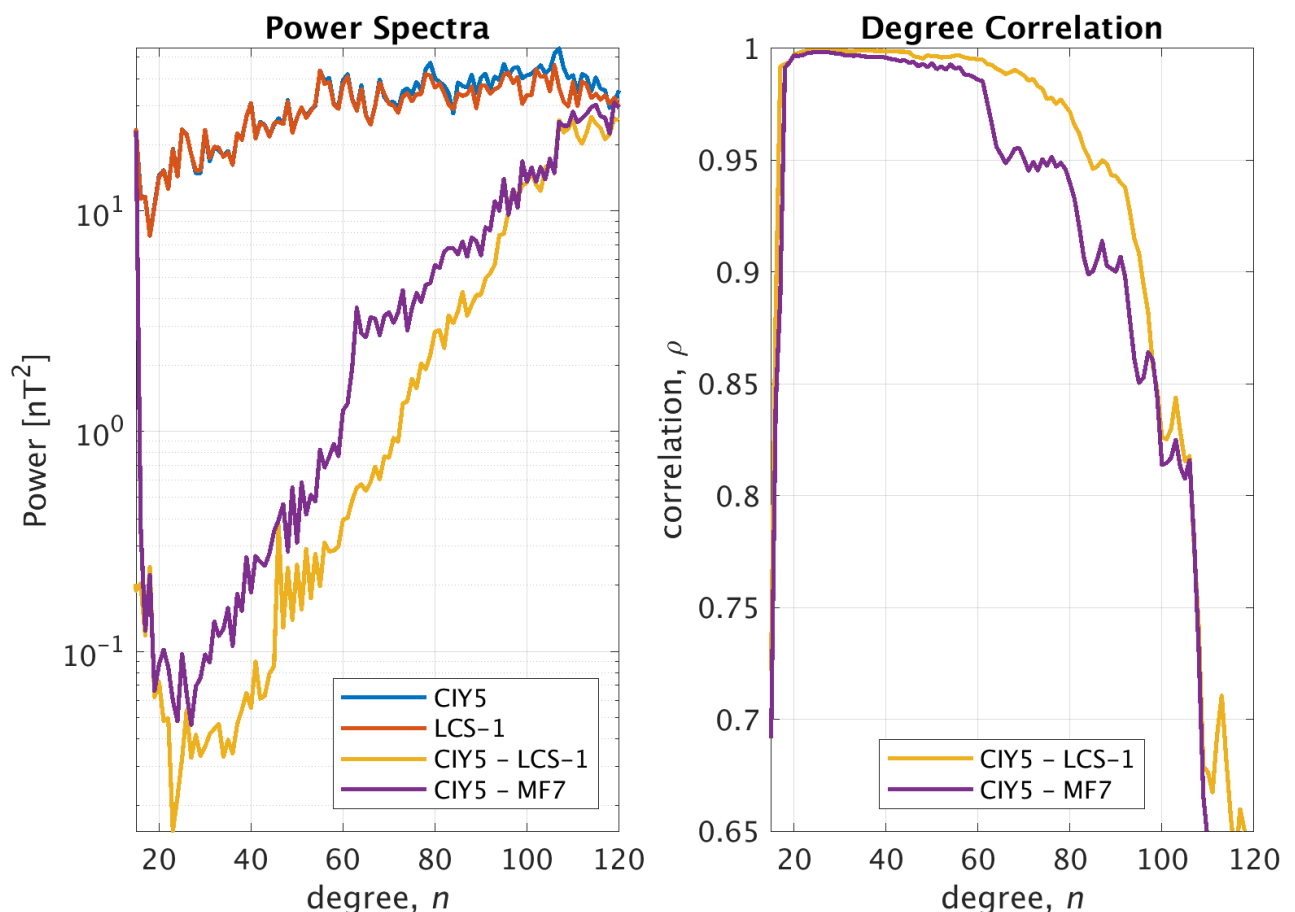


Figure 1-1: Spatial power densities and degree correlations

# Swarm Level 2 Processing System

## 1.4.2 Normalized Spherical Harmonic Coefficient Differences

Figure 1-2 below shows the relative differences in percent between each spherical harmonic coefficient of the CIY5 and the LCS-1 and MF7\* models respectively in degree versus order matrices. These plots show slight differences at lower degree and low order probably due to crosstalk with the ionospheric field, but otherwise the models agree well – in particular the CIY5 and LCS-1 models.

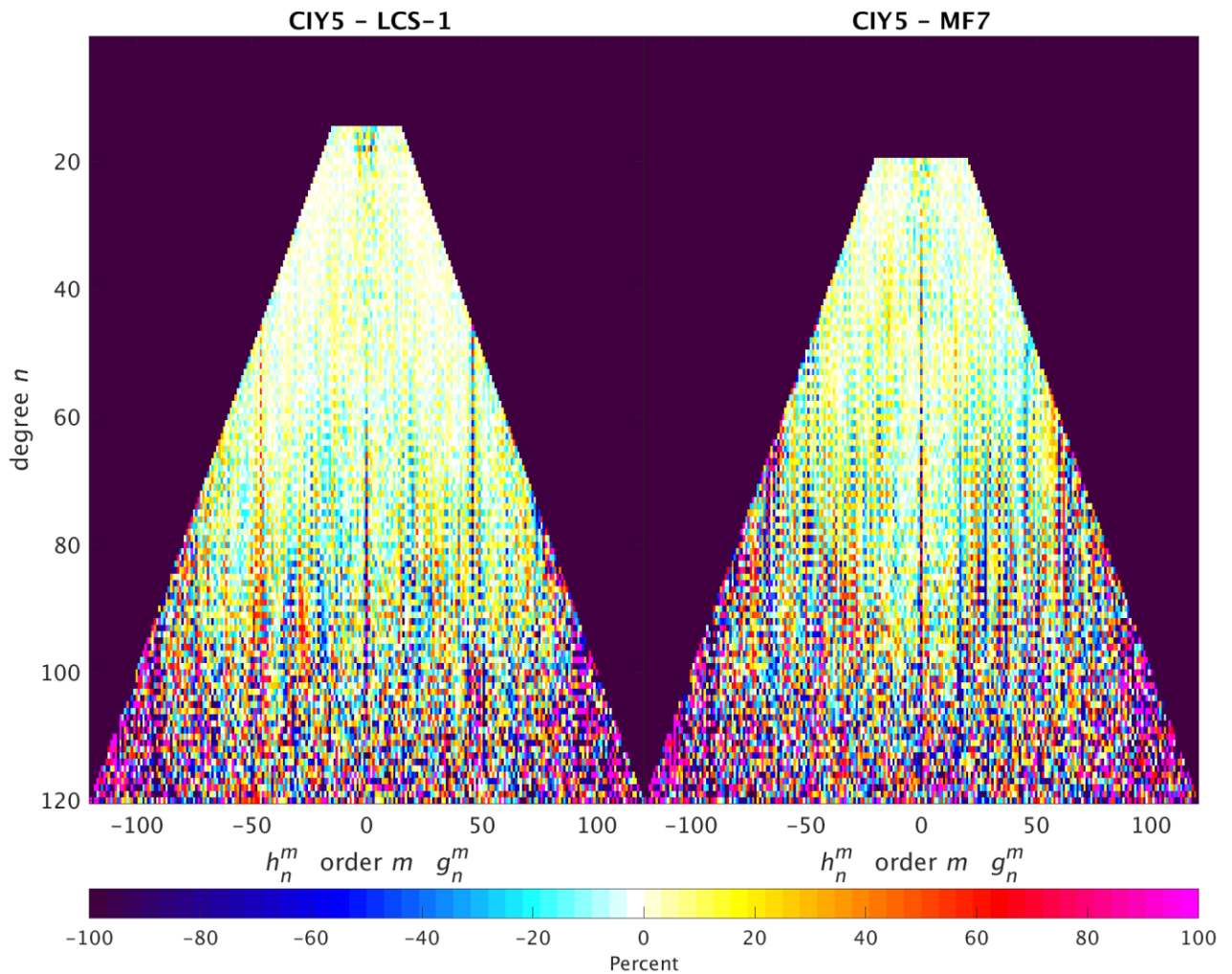


Figure 1-2: Normalized coefficient differences in percent

\* Degrees 20-120

# Swarm Level 2 Processing System

## 1.4.3 Visualisation of Spatial Differences

Figure 1-3 below shows the difference in  $B_r$  between the CIY5 and LCS-1 lithospheric field models at Earth's surface for degrees 15-105 at epoch 2015. These plots reveal the main differences to be in the auroral regions above quasi-dipole latitude  $\pm 55^\circ$  but also show a tendency to “banding” along the satellite tracks though less pronounced than previous years CI models. A “polar gap” artefact also seem to have arisen in particular at the South Pole possible due to the increase in spherical harmonic degree of the model.

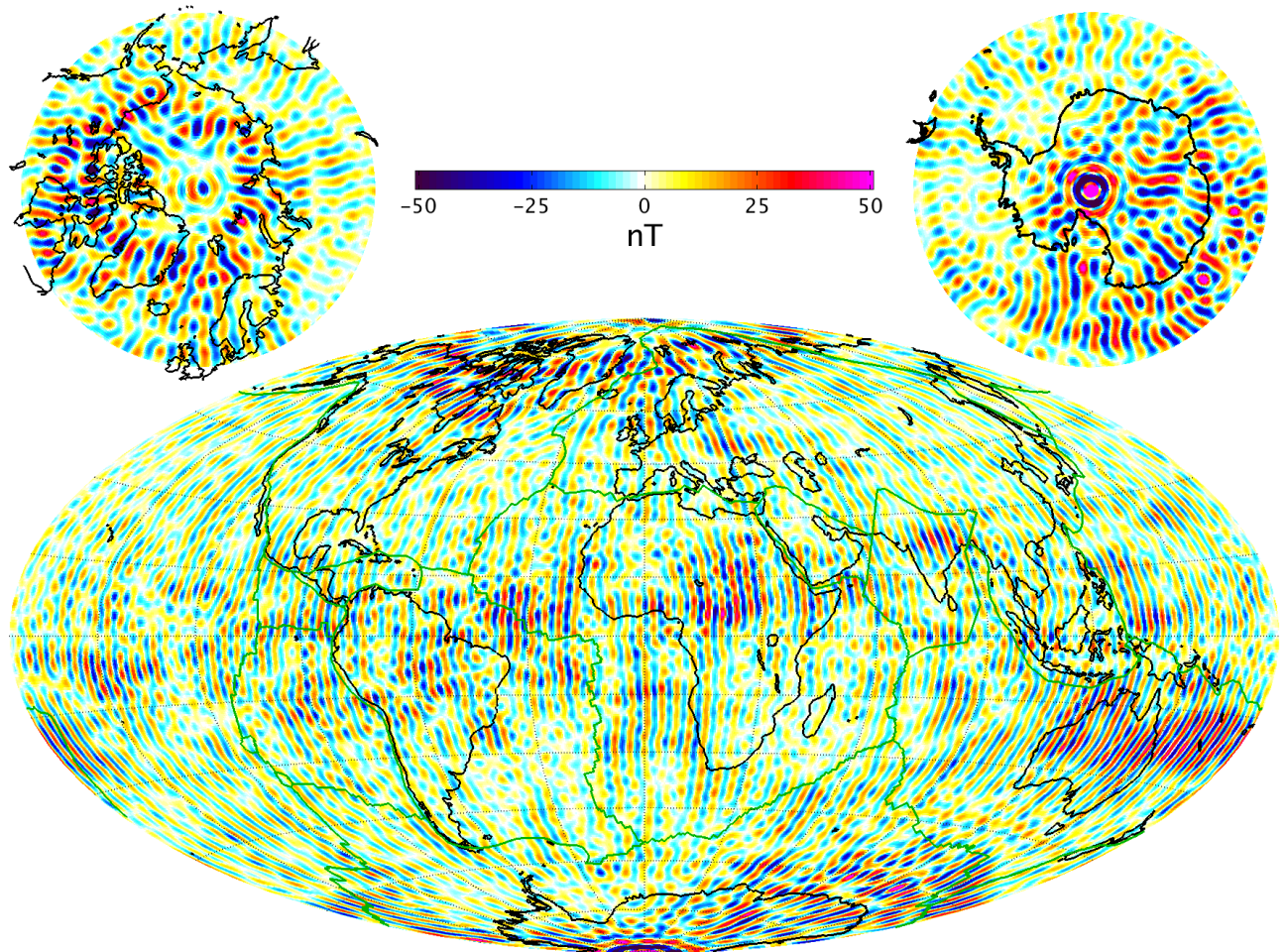


Figure 1-3: Spatial visualization of  $B_r$  differences between CIY5 and LCS-1 models

# Swarm Level 2 Processing System

## 1.4.4 Visualisation of Radial Field

Figure 1-4 below shows the radial field,  $B_r$ , of the CIY5 lithospheric field models at Earth's surface for degrees 15-120 at epoch 2015.

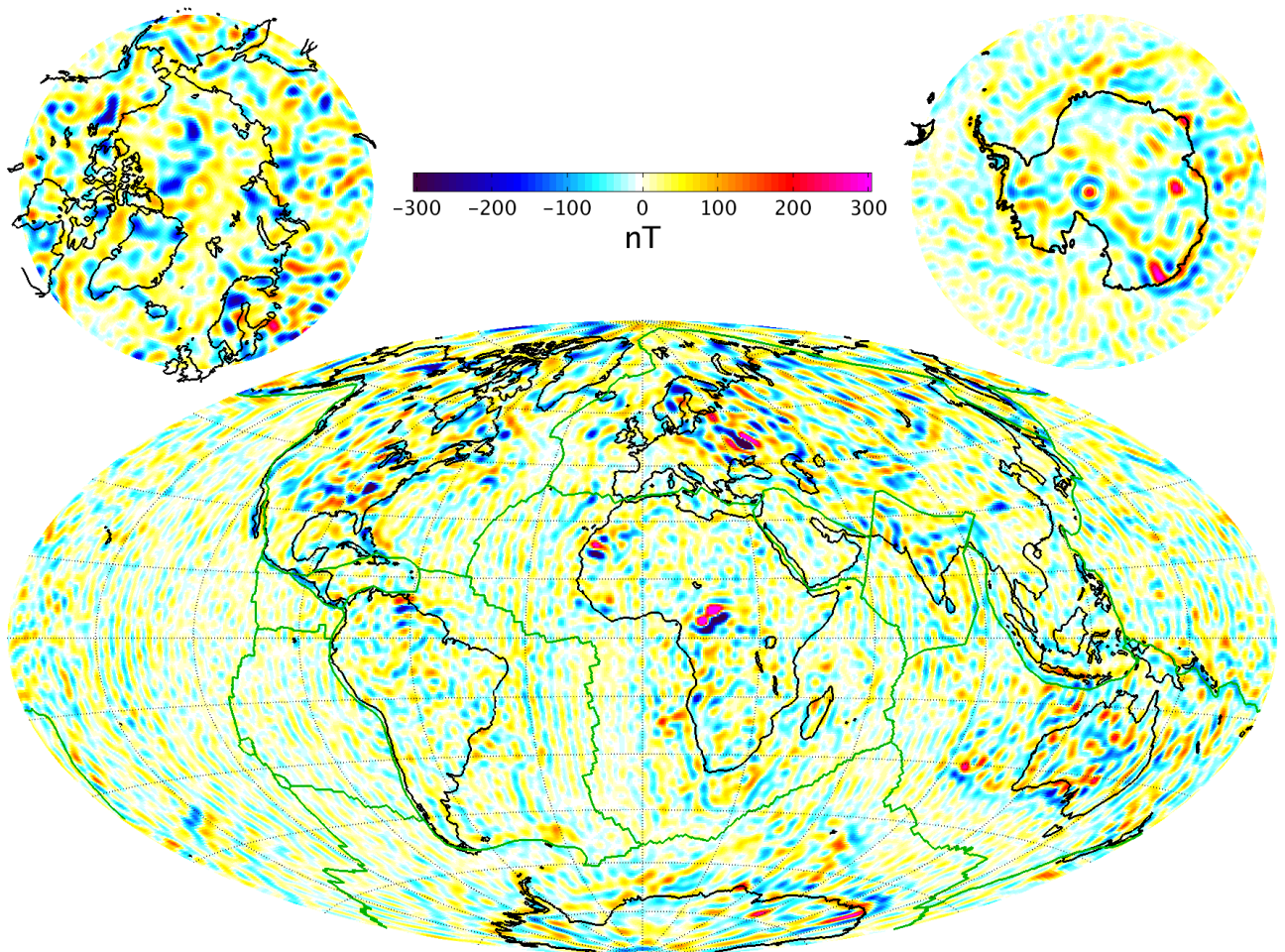


Figure 1-4: Spatial visualization of  $B_r$  of the CIY5 model

## 1.4.5 Statistics of Model Residuals

The statistics of the data residuals obtained by the CIY5 modelling is given in Table 1-2 below. Grey cells indicate data from night side, white cells indicate data from sunlit regions. Crossed cells indicate data which are not used in the inversion process. “Field” indicate the pure vector and scalar measurements, whereas “NS diff” and “EW diff” indicate the North-South (along-track) respectively East-West differences. The standard deviations (of the residuals between the observations and the estimated model) of the differences are quite impressive; the standard deviations of the direct field measurements from the satellites are also remarkably . Note also the almost perfect similarity between Swarm A and C (side-by-side flying pair) and North-South

# Swarm Level 2 Processing System

differences for all three satellites. Swarm B shows slightly higher residuals in the horizontal and scalar Field components ( $B_\theta$ ,  $B_\phi$ , and F) at low and mid latitudes and slightly lower residuals at high latitudes likely due to its higher altitude.

Swarm/ Obs.		Geomagnetic quasi-dipole latitude											
		Low, $\leq 10^\circ$				Mid, $]10^\circ..55^\circ]$				High, $> 55^\circ$			
		Standard deviations of data residuals, weighted, [nT]											
		$\sigma(B_r)$	$\sigma(B_\theta)$	$\sigma(B_\phi)$	$\sigma(F)$	$\sigma(B_r)$	$\sigma(B_\theta)$	$\sigma(B_\phi)$	$\sigma(F)$	$\sigma(B_r)$	$\sigma(B_\theta)$	$\sigma(B_\phi)$	$\sigma(F)$
A	Field	1.63	1.92	1.66	2.41	1.65	2.09	2.07	1.78				5.62
	NS diff	0.31	0.18	0.32	0.16	0.24	0.28	0.35	0.18				0.93
		0.89	0.76	0.79	0.68	0.49	0.53	0.82	0.31				1.05
B	Field	1.64	2.49	1.98	3.29	1.88	2.55	2.26	2.33				5.44
	NS diff	0.30	0.18	0.30	0.16	0.24	0.28	0.34	0.19				0.83
		0.80	0.67	0.72	0.60	0.47	0.52	0.80	0.29				0.95
C	Field	1.64	1.87	1.64	2.38	1.65	2.08	2.07	1.78				5.62
	NS diff	0.32	0.18	0.32	0.16	0.25	0.29	0.35	0.18				0.93
		0.90	0.76	0.78	0.68	0.49	0.54	0.82	0.31				1.05
A-C	EW diff	0.55	0.40	0.74	0.36	0.38	0.44	0.75	0.32				0.55
		1.22	0.63	1.79	0.51	0.70	0.75	1.50	0.44				0.59
Magnetic observatories		3.99	4.01	4.50	n.c.	3.44	3.87	4.31	n.c.	13.23	12.83	10.41	n.c.
		11.41	13.43	9.39	n.c.	5.31	6.75	7.97	n.c.	16.26	17.37	15.07	n.c.

Table 1-2: Statistics of model residuals

## 1.5 Criteria

Table 1-3 below summarizes the criteria used to check the validity of the MLI\_SHAi2C product:

Input	Test	Criteria	Pass?
Observations	Residual statistics	Standard deviation of vector data below 7 nT.	Ok
Alternative model	Comparison with model	CI model agrees with alternative model	Ok

Table 1-3: Validation criteria

# Swarm Level 2 Processing System

## 2 Additional Information

### 2.1 Model Configuration and Data Selection Parameters

The MLI\_SHAi2C product is obtained as a comprehensive co-estimation of the core, lithosphere, ionosphere, and magnetosphere field contributions including induced contributions similar to the method described in [Sabaka et.al., GRL, 2016]. The complete model configuration used is given in Table 2-1 below; the MLI\_SHAi2C product is the green part:

Model Part	Maximum Degree/Order	Temporal Characteristics	Comment
Core	18/18	Order 5 B-spline with knots every 6 months	Damping of the mean-square, second and third time derivatives of $B_r$ at the core-mantle boundary (at 3480 km radius) with enhanced damping of zonal terms up to degree 9.
Lithosphere	120/120	Static	Degree 19-120 purely determined by North-South differences from all satellites and East-West differences of lower pair satellite (A and C).  Damping of $B_r$ for degrees 91 and above to reduce noise
Ionosphere	45/5 (dipole coordinates)	Annual, semi-annual, 24-, 12-, 8- and 6- hours periodicity	Spherical harmonic expansion in quasi-dipole (QD) frame, underlying dipole SH $n_{max} = 60$ , $m_{max} = 12$ . Scaling by 3-months averages of F10.7 plus induction via a priori 3-D conductivity model (“1-D+oceans”) and infinite conductor at depth.  Damping of: <ol style="list-style-type: none"><li>1. Mean-square current density <math>J</math> in the E-region within the nightside sector (magnetic local times 21:00 through 05:00; peak damping at 01:00)</li><li>2. Mean-square of the surface Laplacian of <math>J</math> multiplied by a factor of <math>\sin^8(2\theta)</math> over all local times, where <math>\theta</math> is co-latitude.</li></ol>

# Swarm Level 2 Processing System

Model Part	Maximum Degree/Order	Temporal Characteristics	Comment
Magnetosphere, external	3/1	One hour bins	
Magnetosphere, induced	3/3	One hour bins	
M2 Tidal	18/18	Periodicity: 12.42060122 hr, phase fixed with respect to 00:00:00, 1999 January 1 GMT	

Table 2-1: Model Configuration

The data selection criteria are:

- Coarse agreement with CHAOS-6 field model:  $\Delta B_c \leq 500$  nT for all components  $c=r,\theta,\phi$ , and  $\Delta F \leq 100$  nT.
- $K_p \leq 3^0$  for gradient data,  $K_p \leq 2^-$  for field data
- Time-derivative of Dst:  $|dDst/dt| \leq 3$  nT/hour
- 30 second satellite sampling period, NS gradient data computed from 15 second differences
- core and tidal fields determined from night-side data only, i.e. with Sun  $\geq 10^\circ$  below the horizon

## 2.2 Comments from Scientists in the Loop

### 2.2.1 Derivation of Model

The final Comprehensive Inversion model using five years of Swarm data shows very good agreement with alternative models and excellent residual statistics (Table 1-2). Slight along-track banding and differences in polar regions are observed when comparing to other models (see Figure 1-3).

### 2.2.2 Conclusion

The estimated model is assessed to be of good quality with very good agreement with alternative lithospheric field models.

## Annex A Definitions of Tests

### A.1 Mean square vector field difference per spherical harmonic degree

The mean square vector field difference between models per spherical harmonic degree ( $n$ ) is diagnostic of how closely the models match on average across the globe. The difference between Gauss coefficients  $g_n^m$  of model  $i$  and model  $j$  can be defined as:

$${}_{i,j}R_n = (n+1) \left( \frac{a}{r} \right)^{(2n+4)} \sum_{m=0}^n [{}_i g_n^m - {}_j g_n^m]^2$$

Equation A-1

where  $n$  is the degree,  $m$  is the order,  $a$  is the magnetic reference spherical radius of 6371.2 km which is close to the mean Earth radius, and  $r$  is the radius of the sphere of interest, which is taken as  $r = a$  for comparisons at the Earth's surface and  $r = 3480$  km for comparisons at the core-mantle boundary.

Summing over degrees  $n$  from 1 to the truncation degree  $N$  and taking the square root yields the RMS vector field difference between the models  $i$  and  $j$  averaged over the spherical surface:

$${}_{i,j}R = \sqrt{\sum_{n=1}^N {}_{i,j}R_n}$$

Equation A-2

### A.2 Correlation per spherical harmonic degree

Analysis of spherical harmonic spectra is a powerful way to diagnose differences in amplitude between models but tells us little about how well they are correlated. The correlation per degree between two models again labelled by the indices  $i$  and  $j$  can be studied as a function of spherical harmonic degree using the quantity:  ${}_{i,j}\rho_n$

$${}_{i,j}\rho_n = \frac{\sum_{m=0}^n ({}_i g_n^m {}_j g_n^m)}{\sqrt{\left( \sum_{m=0}^n ({}_i g_n^m)^2 \right) \left( \sum_{m=0}^n ({}_j g_n^m)^2 \right)}}$$

Equation A-3

Ideally, the correlation should be close to 1 for all models, indicating that they have equivalent features and coefficients. If the correlation falls below 0.5, for degrees 1-9, then the models should be examined in more detail. Coefficients from degree 10-13 in IGRF and WMM are less well-determined (e.g. due to noise) and also change more rapidly so are not expected to be well correlated by the launch of the Swarm mission.

### A.3 Visualisation of coefficient differences

A final method of visualising the differences in Gauss coefficients is to plot the differences  ${}_i g_n^m - {}_j g_n^m$  as a triangular plot, with the zonal coefficients lying along the centre of the triangle, the sectorial coefficients along the edges and the tesseral coefficients filling the central regions. These plots will illustrate which, if any, coefficients are strongly divergent between models

# Swarm Level 2 Processing System

## A.4 Visualisation of spatial differences

A geographical investigation of the models can be made by plotting the differences in the  $B_x$ ,  $B_y$  and  $B_z$  components of the field at Earth surface (approximated by ellipsoid). Studying differences between the Swarm models and reference models in space yields insight into the geographical locations where disparities are located, illustrating whether biases or errors have arisen in certain regions (e.g. polar areas).

.